The Astrophysical Journal, 597:1036–1048, 2003 November 10

THE GALACTIC POPULATION OF LOW- AND INTERMEDIATE-MASS X-RAY BINARIES

Eric Pfahl,[1] Saul Rappaport,[2] and Philipp Podsiadlowski[3]
Received 2003 March 21; accepted 2003 July 16

ABSTRACT

We present the first study that combines binary population synthesis in the Galactic disk and detailed evolutionary calculations of low- and intermediate-mass X-ray binaries (L/IMXBs). Our approach allows us to follow completely the formation of incipient L/IMXBs and their evolution through the mass-transfer phase to the point when they become binary millisecond pulsars (BMPs). We show that the formation probability of IMXBs with initial donor masses of 1.5–4 $M_\odot$ is typically $\gtrsim 5$ times higher than that of standard LMXBs with initial donor masses of less than 1.5 $M_\odot$. Since IMXBs evolve to resemble observed LMXBs, we suggest that the majority of the observed systems may have descended from IMXBs. Distributions at the current epoch of the orbital periods, donor masses, and mass accretion rates of L/IMXBs have been computed, as have orbital-period distributions of BMPs. This is a major step forward over previous theoretical population studies of L/IMXBs that utilized only crude representations of the binary evolution through the X-ray phase. Several significant discrepancies between the theoretical and observed distributions are discussed. We find that the total number of luminous ($L_X > 10^{36}$ ergs s^{-1}) X-ray sources at the current epoch and the period distribution of BMPs are very sensitive to the parameters in the analytic formula describing the common-envelope phase that precedes the formation of the neutron star. The orbital-period distribution of observed BMPs strongly favors cases in which the common envelope is more easily ejected. However, this leads to an approximately hundred-fold overproduction of the theoretical number of luminous X-ray sources relative to the total observed number of LMXBs. As noted by several groups prior to our study, X-ray irradiation of the donor star may result in a dramatic reduction in the X-ray active lifetime of L/IMXBs, and we suggest that irradiation may resolve the overproduction problem as well as the long-standing BMP/LMXB birthrate problem.

Subject headings: binaries: close — pulsars: general — stars: neutron — X-rays: stars

1. INTRODUCTION

Roughly 140 low-mass X-ray binaries (LMXBs) are known in the Galaxy (Liu, van Paradijs, & van den Heuvel 2001), with orbital periods from 11 minutes to ~1 yr, donor masses of ~0.01–2 $M_\odot$, and X-ray luminosities from the detection sensitivities to ~10^{38} ergs s^{-1}. Over the past 20 years or so, many theoretical studies of LMXBs have aimed at accounting for their abundance and variety. During this time, a standard picture for the formation and evolution of LMXBs in the Galactic disk has emerged. However, recent observational and theoretical work has challenged the conventional wisdom and prompted a renewed interest in the origins of observed LMXBs. Specifically, it has been realized that many, perhaps even the majority, of the identified LMXBs with low-mass stellar companions may be descendants of systems with *intermediate-mass* ($\gtrsim 1.5$ $M_\odot$) donor stars.

In the past, all binary population synthesis studies that explicitly considered the evolution of X-ray binaries and the criteria for dynamically unstable mass transfer involved analytic approximations (e.g., Rappaport, Joss, & Webbink 1982; Kalogera & Webbink 1996; King & Ritter 1999). This is a satisfactory approach as long as the structure of the donor star and its response to mass loss can be described using relatively simple prescriptions; however, this is not possible in general. The clear and widespread realization that intermediate-mass donor stars can stably transfer matter to a neutron star (NS) accretor came largely as a result of recent calculations that utilized full stellar evolution codes (e.g., Tauris & Savonije 1999; Podsiadlowski & Rappaport 2000; Tauris, van den Heuvel, & Savonije 2000; Kolb et al. 2000; Podsiadlowski, Rappaport, & Pfahl 2002). Only with such codes can the evolution of the donor be followed realistically during the rapid phase of thermal timescale mass transfer that characterizes the early evolution of intermediate-mass X-ray binaries (IMXBs).

Podsiadlowski et al. (2002, hereafter Paper I) is devoted to a systematic evolutionary study of L/IMXBs, wherein we describe a library of 100 evolutionary sequences computed with a standard Henyey-type stellar structure code. This library has now been expanded to 144 sequences, covering initial orbital periods from 2 hr to 100 days and initial donor masses from 0.3 to 7 $M_\odot$. The library is intended to provide fairly complete coverage of the initial conditions that are likely to be encountered in a population synthesis study of L/IMXBs.

Here we extend the work in Paper I by combining our library with a detailed Monte Carlo binary population synthesis (BPS) code for L/IMXBs. The code includes standard assumptions for the population of massive primordial binaries, reasonable analytic prescriptions to describe both stable and dynamically unstable mass transfer prior to the supernova (SN) explosion, and NS kicks. Similar codes are described in Portegies Zwart & Verbunt (1996) and Belczynski, Kalogera, & Bulik (2002). We undertake a limited exploration of the set of free parameters that enters

[1] Chandra Fellow; Harvard-Smithsonian Center for Astrophysics, 60 Garden Street, Cambridge, MA 02138; epfahl@cfa.harvard.edu.
[2] Center for Space Research, Massachusetts Institute of Technology, Cambridge, MA, 02139; sar@mit.edu.
[3] Department of Astrophysics, Oxford University, Oxford, OX1 3RH, England, UK; podsi@astro.ox.ac.uk.

the BPS calculation used to generate the incipient X-ray binaries. Most important are the parameters that describe the distribution of NS kick speeds and the outcome of common-envelope evolution. For reasonable variation of the uncertain parameters of our study, the formation probability of L/IMXBs ranges over 2 orders of magnitude.

For each incipient L/IMXB that emerges from the BPS calculation, we find an initial model in our library with the closest matching orbital period and donor mass. For the ensemble of selected sequences, we apply a temporal weighting scheme along the evolutionary tracks to calculate the distributions of potentially observable quantities at the current epoch. This is the first paper where such distributions have been computed for L/IMXBs, and it is now possible to directly compare population models and the statistics of observed systems.

The paper is organized as follows. In § 2, we briefly describe our BPS code, highlighting the important uncertainties and the associated free parameters. The population of incipient X-ray binaries that emerges from the BPS calculation is discussed in § 3. Key results of this study are presented in § 4, where we show distributions of various quantities at the current epoch and make rough comparisons with the observational data. Several topics related to L/IMXB evolution, including binary millisecond pulsars and X-ray irradiation, are addressed in § 5. Finally, in § 6, the most important results of our investigation are listed along with suggestions for how this work may be extended and improved.

2. MASSIVE BINARY POPULATION SYNTHESIS

The formation of a NS in a binary system involves three main evolutionary steps: (1) the formation of a primordial binary, where the initially more massive component (the primary) has a mass $\gtrsim 8\ M_\odot$, (2) a phase of mass transfer from the primary to the secondary (the initially less massive component), and (3) the subsequent SN explosion of the primary's hydrogen-exhausted core and the formation of the NS. Our Monte Carlo BPS code utilizes a set of simple, but adequate, analytic prescriptions to describe each of these steps. Given the significant uncertainties associated with L/IMXB formation, a more sophisticated and computationally intensive treatment is probably not warranted at the present time. In § 3 and § 4, we indicate graphically and in tabular form how changes in the most important parameters of our study affect our results. We now give a brief overview of the important elements of our BPS code: an expanded account is provided in Pfahl, Rappaport, & Podsiadlowski (2002).

2.1. *Primordial Binaries*

We construct each primordial binary by selecting the component masses and orbital parameters from the following distribution functions.

Primary Mass.—The initial primary mass, M_{1i}, is chosen from a power-law initial mass function, $p(M_{1i}) \propto M_{1i}^{-x}$. We use a fixed value of $x = 2.5$ for massive stars (Miller & Scalo 1979; Scalo 1986; Kroupa, Tout, & Gilmore 1993). Primary masses are restricted to the range $M_{1i} = 8$–$25\ M_\odot$, and we assume that the primary is always the NS progenitor (see, however, Podsiadlowski, Joss, & Hsu 1992; Pols 1994; Wellstein, Langer, & Braun 2001).

Secondary Mass.—The initial secondary mass, M_{2i}, is chosen from a distribution in mass ratios, $p(q_i) \propto q_i^y$, where $q_i \equiv M_{2i}/M_{1i} < 1$. Strongly motivated by the work of Garmany, Conti, & Massey (1980), we prefer a flat distribution ($y = 0$), but we also consider $y = -1$ and $y = +1$.

Eccentricity.—Without much loss in generality, we take the primordial binary orbits to be circular. This assumption is discussed in Pfahl et al. (2002).

Semimajor Axis.—The initial orbital separation, a_i, is drawn from a distribution that is uniform in $\log a_i$ (Abt & Levy 1978). We determine the minimum value of a_i for each system by demanding that neither star overflows its Roche lobe on the main sequence. The upper limit is somewhat arbitrary, but here is taken to be 10^3 AU.

2.2. *Mass Transfer*

If $a_i \lesssim 5$–10 AU, the primary will grow to fill its Roche lobe at some point during its evolution. The subsequent phase of mass transfer is of crucial importance in determining what types of NS binaries are ultimately produced. It is common practice to distinguish among three main evolutionary phases of the primary at the onset of mass transfer (Kippenhahn & Weigert 1967; Podsiadlowski et al. 1992). Case A evolution corresponds to core hydrogen burning, case B refers to the shell hydrogen-burning phase, but prior to central helium ignition, and case C evolution begins after core helium burning. It is quite improbable for mass transfer to begin during core helium burning, and we thus neglect this possibility (see Pfahl et al. 2002). We refer to as case D the large fraction of wide binaries that remain detached prior to the SN explosion of the primary. Using the distributions and standard-model parameters given above as well as the treatment of stellar winds discussed below, we find that cases A, B, C, and D comprise roughly 5%, 30%, 15%, and 50%, respectively, of the primordial binary population. The case for each binary is found using the single-star evolution fitting formulae of Hurley, Pols, & Tout (2000).

Mass transfer from the primary to the secondary may be *stable* or *dynamically unstable*, depending mainly on the binary mass ratio and evolutionary state of the primary when it fills its Roche lobe. In our population study of L/IMXBs, we consider only case B and case C mass transfer. Case A mass transfer accounts for only a small fraction of the binaries and, furthermore, most likely leads to the merger of the two stars following a contact phase (Wellstein et al. 2001). Most case D systems are disrupted because of the SN explosion of the primary if NS kicks are significant. We do not consider case D systems that survive the SN; for a discussion of the products that may emerge from this evolutionary channel, see Kalogera (1998) and Willems & Kolb (2002).

Cases B and C are divided into *early* (B_e or C_e) and *late* (B_l or C_l) phases if the primary has an envelope that is mostly radiative or deeply convective, respectively. We assume that mass transfer is stable, though nonconservative, for cases B_e and C_e if the mass ratio, after any wind mass loss has occurred, is greater than q_c, where q_c is some critical mass ratio. We adopt a fixed value of $q_c = 0.5$ in our study (Wellstein et al. 2001). If the primary has a deep convective envelope when it fills its Roche lobe, mass transfer is dynamically unstable and a common-envelope (CE) phase ensues, which results in either a very compact binary or a merger.

A single star of mass $\gtrsim 15\ M_\odot$ may lose $\gtrsim 30\%$ of its mass in a stellar wind during the red supergiant phase. For stars of mass $\lesssim 25\ M_\odot$, only $\lesssim 5\%$ of the mass is lost on the main sequence. We suppose that the wind from the primary in a binary system takes with it the specific orbital angular momentum of the star. In response to the red supergiant winds, the Roche lobe of the primary expands and may overtake the expansion of the star, making Roche lobe overflow and case C_l mass transfer impossible. We have included the effects of stellar winds only for initial primary masses greater than 13 $M_\odot$ both on the main sequence and while the star is a red supergiant: our procedure is similar to the one adopted by Podsiadlowski, Rappaport, & Han (2003). For this range of masses, core helium burning begins while the star is in the Hertzsprung gap, and there is no decrease in the stellar radius. Primaries of mass $M_{1i} \lesssim 13\ M_\odot$ experience moderate wind mass loss during core helium burning following evolution through the first giant branch, but the stellar radius decreases after helium ignition, precluding Roche lobe overflow during this phase. We note that the mass that separates the two behaviors just mentioned is actually quite uncertain (Langer & Maeder 1995) and may be as large as $\sim 20\ M_\odot$.

If a merger is avoided, it is reasonable to suppose that the primary loses its entire envelope, leaving only its hydrogen-exhausted core, irrespective of whether mass transfer is stable or dynamically unstable. Following case B mass transfer, the mass of the helium core is given approximately by (Hurley et al. 2000)

$$M_{c,i} \simeq 0.1 M_{1i}^{1.35}\ , \tag{1}$$

where $M_{c,i}$ and M_{1i} are in units of solar masses. We neglect the relatively small amount of wind mass loss on the main sequence and use the initial mass of the primary to compute the initial core mass $M_{c,i}$ before it, too, loses mass in a wind. The mass of the exposed core may be larger by ~ 0.5–$1\ M_\odot$ after case C mass transfer as a result of shell nuclear burning. A helium core will ultimately yield an NS remnant if its mass is $\gtrsim 2\ M_\odot$ (Habets 1986b). Equation (1) gives a primary mass threshold for NS formation of $\sim 9\ M_\odot$.

For our chosen maximum primary mass of 25 $M_\odot$, the corresponding core mass is $\sim 8\ M_\odot$. A nascent helium star of mass 3–8 $M_\odot$ that is exposed following case B mass transfer may lose 10%–30% of its mass in a wind before the SN (Brown et al. 2001; Pols & Dewi 2002). The final core mass is related to the initial helium star mass by the approximate formula (see Fig. 1 of Pols & Dewi 2002)

$$M_{c,f} \sim 1.4 M_{c,i}^{2/3}\ , \tag{2}$$

for $M_{c,i} \gtrsim 3\ M_\odot$. Following case C mass transfer, the core of the primary has already undergone helium burning, and there is insufficient time for winds to significantly reduce its mass.

If $M_{c,i} \lesssim 3\ M_\odot$ following case B mass transfer, we may safely neglect winds, but such helium stars may expand to giant dimensions following core helium burning, often initiating a phase of so-called case BB mass transfer to the secondary (De Greve & De Loore 1977; Delgado & Thomas 1981; Habets 1986a). We do not attempt to model this evolution in detail but simply assume that $0.5\ M_\odot$ is transferred conservatively from the primary's core to the secondary. In case BB systems where $M_{2i} < M_{c,i}$, such as when the secondary is of low or intermediate mass, the mass transfer may proceed on the thermal timescale of the core, and the evolution may be quite complicated (Dewi et al. 2002; Ivanova et al. 2003). However, any reasonable treatment of case BB mass transfer is not likely to change our results for L/IMXBs substantially,

Stable mass transfer from the primary to the secondary is treated analytically as follows. We assume that the secondary accretes a fraction β of the material lost from the primary during Roche lobe overflow. The complementary mass fraction, $1 - \beta$, escapes the system with specific angular momentum α in units of the orbital angular momentum per unit of reduced mass. We use constant values of $\alpha = 1.5$, characteristic of mass loss through the L2 point, and $\beta = 0.75$. The final orbital separation is then given by the generic equation (Podsiadlowski et al. 1992)

$$\left(\frac{a'}{a}\right)_{\rm RLO} = \frac{M_b'}{M_b}\left(\frac{M_1'}{M_1}\right)^{C_1}\left(\frac{M_2'}{M_2}\right)^{C_2}\ , \tag{3}$$

where

$$\begin{aligned} C_1 &\equiv 2\alpha(1-\beta) - 2\ , \\ C_2 &\equiv -2\alpha(1-\beta)/\beta - 2\ . \end{aligned} \tag{4}$$

Here the subscript RLO denotes stable Roche lobe overflow, and unprimed and primed quantities denote parameters at the onset and termination of mass transfer, respectively.

It is easily verified that, in our simulations, the *minimum* secondary mass resulting from stable mass transfer is roughly $q_c\ 8\ M_\odot + \beta\ 6\ M_\odot$, where $8\ M_\odot$ is the minimum primary mass and $6\ M_\odot$ is the corresponding envelope mass shed during mass transfer. For our chosen values of $q_c = 0.5$ and $\beta = 0.75$, this minimum mass is $8.5\ M_\odot$, considerably larger than the maximum initial donor mass of $\sim 4\ M_\odot$, for which an IMXB undergoes stable mass transfer (see Paper I). Thus, in our work, all incipient L/IMXBs are the products of dynamically unstable mass transfer.

We use the conventional energy relation to describe the dynamical spiral-in during a CE phase (Webbink 1984). The ratio of the final to the initial orbital separation is given by the generic equation

$$\left(\frac{a'}{a}\right)_{\rm CE} = \frac{M_c M_2}{M_1}\left(M_2 + \frac{2M_e}{\lambda_{\rm CE}\ \eta_{\rm CE}\ r_{\rm L1}}\right)^{-1}\ , \tag{5}$$

where $r_{\rm L1}$ is the Roche lobe radius of the primary in units of the orbital separation, M_e and M_c are the masses of the primary's envelope and core, respectively, $\lambda_{\rm CE}$ parameterizes the structure of the envelope, and $\eta_{\rm CE}$ is the fraction of orbital binding energy that goes into dissipating the envelope. Although $\lambda_{\rm CE}$ and $\eta_{\rm CE}$ appear only in the product $\lambda_{\rm CE}\ \eta_{\rm CE}$, we suppose, without loss of generality, that $\eta_{\rm CE} = 1$ and fix $\lambda_{\rm CE}$ in the range 0.1–0.5 for each simulation. In reality, $\lambda_{\rm CE}$ changes as a star evolves, typically decreasing to $\lesssim 0.1$–0.2 as the massive star passes through the Hertzsprung gap and increasing to ~ 0.1–0.4 following core He burning (Dewi & Tauris 2000, 2001). Generally, $\lambda_{\rm CE}$ decreases for all stellar radii as the mass of the star is increased. Equation (5) gives typical shrinkage factors of $(a'/a)_{\rm CE} \sim 0.01$ for systems with low- and intermediate-mass secondaries.

A sufficient condition for the merger of the primary and secondary is that the main-sequence secondary overfills its

Roche lobe for the calculated post-CE orbital separation. Therefore, the minimum separation for surviving systems must be larger than several solar radii, corresponding to initial orbital separations greater than several *hundred* solar radii. It turns out that the majority of the dynamically unstable case B_e and C_e systems merge following the CE, and that for most systems that survive the CE, the primary is a convective red supergiant (case B_l or C_l) at the onset of mass transfer.

2.3. *Supernova Explosion*

After the exposed core of the primary consumes its remaining nuclear fuel, it explodes as a Type Ib or Ic SN and leaves an NS remnant. We take the initial NS mass to be 1.4 $M_\odot$. Impulsive mass loss and the NS kick strongly perturb the binary and may cause its disruption. Mass loss is especially significant, since the mass ejected may be comparable to or greater than the secondary mass. Some important insights can be obtained rather simply by neglecting NS kicks.

It is straightforward to show (Blaauw 1961; Boersma 1961) that for a circular pre-SN orbit and *vanishing kicks*, the eccentricity, $e_{\rm SN}$, after the SN is simply

$$e_{\rm SN} = \frac{M_c - M_{\rm NS}}{M_2 + M_{\rm NS}} , \qquad (6)$$

where $M_{\rm NS}$ is the mass of the NS, and M_c is the preexplosion core mass. The system is unbound when $M_c > M_2 + 2M_{\rm NS}$. Letting $M_2 = 1\ M_\odot$, we see that for $M_c > 3.8\ M_\odot$ ($M_1 \gtrsim 15\ M_\odot$), disruption of the binary is guaranteed. A kick of appropriate magnitude and direction is then *required* in order to keep the system bound. For intermediate-mass secondaries, a wider range of pre-SN core masses is permitted when kicks are neglected. Equation (6) gives values of $e_{\rm SN} \gtrsim 0.5$ for some typical core and secondary masses. Following the CE phase, the core of the primary will have orbital speeds about the binary center of mass (CM) of $v_c \gtrsim 200$ km s^{-1}. After the SN, mass loss alone gives the binary CM a speed of $v_{\rm CM} = e_{\rm SN} v_c$, so that eccentricities of $e_{\rm SN} \gtrsim 0.5$ correspond to large post-SN systemic speeds on the order of 100 km s^{-1}.

When NS kicks are considered in addition to SN mass, a larger fraction of systems are disrupted, and those binaries that do remain bound will have larger CM speeds. We utilize a Maxwellian distribution in kick speeds,

$$p(v_k) = \sqrt{\frac{2}{\pi}} \frac{v_k^2}{\sigma_k^3} \exp\left(-\frac{v_k^2}{2\sigma_k^2}\right) , \qquad (7)$$

where the directions of the kicks are distributed isotropically. Dispersions of $\sigma_k \sim 100$–200 km s^{-1} are reasonably consistent with the data on pulsar proper motions (Hansen & Phinney 1997; Arzoumanian, Chernoff, & Cordes 2002). However, neither the functional form of the kick distribution nor the mean are very well constrained. In our study, we consider $\sigma_k = 50$, 100, and 200 km s^{-1}. The post-SN orbital parameters are calculated using the formalism described in Appendix B of Pfahl et al. (2002).

Significant SN mass loss and large NS kicks yield bound post-SN binaries with high eccentricities. Given the post-SN eccentricity, we check if the radius of the secondary is more than 10% larger than its tidal radius at periastron. If this occurs, we assume that the NS immediately spirals into the envelope of the unevolved secondary and do not consider the system further. Our 10% overflow restriction allows for the possibility that tidal circularization and perhaps some mass loss will prevent the objects from merging. The details of eccentric binary evolution with mass transfer is well beyond the scope of this investigation. However, we note in passing that Cir X-1 is most likely a young, possibly intermediate-mass, X-ray binary undergoing episodic mass transfer as a result of having a highly eccentric ($e_{\rm SN} \gtrsim 0.8$) orbit (Shirey 1998).

If the coalescence of the NS and secondary is avoided, we neglect mass loss from the system and assume, rather simplistically, that the binary circularizes while conserving orbital angular momentum. The final orbital separation is then $a_{\rm SN}(1 - e_{\rm SN}^2)$, where $a_{\rm SN}$ is the semimajor axis after the SN. Moreover, we assume that the secondary rotates synchronously with the circularized orbit.

3. INCIPIENT X-RAY BINARIES

The output of the population synthesis calculation is a set of circular binaries, each identified by its orbital period and the mass of the secondary. In order to select initial models from our library of L/IMXB evolutionary sequences, we require the orbital period at which the secondary first fills its Roche lobe. Hereafter, we denote the donor and accretor (NS) masses *in units of* $M_\odot$ by M_d and M_a, respectively.

Orbital angular momentum losses via gravitational radiation (GR) and magnetic braking (MB) may cause the binary separation to decrease substantially prior to mass transfer. The timescale for orbital shrinkage due to GR is

$$\tau_{\rm GR} \simeq 110\ {\rm Gyr}\ q^{-1}(1+q)^{1/3}\left(\frac{P_{\rm orb}}{1\ {\rm day}}\right)^{8/3} , \qquad (8)$$

where $q = M_d/M_a$ and $M_a = 1.4$. We utilize the same standard MB formula as in Paper I (Verbunt & Zwaan 1981; Rappaport, Joss, & Verbunt 1983), with a characteristic timescale given by

$$\tau_{\rm MB} \simeq 3.5\ {\rm Gyr}\ \eta_{\rm MB}^{-1}(1+q)^{-1/3} R_d^{-4}\left(\frac{P_{\rm orb}}{1\ {\rm day}}\right)^{10/3} , \qquad (9)$$

where R_d is the radius of the secondary in solar units, and we introduce $\eta_{\rm MB}$ to parameterize the strength of MB prior to mass transfer. Only when the secondary is strongly tidally coupled to the orbit does MB efficiently extract orbital angular momentum. In an ad hoc way, we let $\eta_{\rm MB} = 0$ or 1 to model the cases in which the tidal coupling prior to Roche lobe overflow is very weak or very strong, respectively. We apply MB only if $0.4 < M_d < 1.5$: less massive stars are fully convective and may not undergo MB (Rappaport et al. 1983), while more massive stars have radiative envelopes and may not undergo MB. When the main-sequence lifetime of a low-mass star exceeds the $\simeq$13 Gyr age of the Galaxy, MB or GR are *required* to drive the system into contact. Intermediate-mass secondaries have nuclear lifetimes of $\sim$0.1–3 Gyr and so do not suffer from this obstacle.

The single-star evolution code of Hurley et al. (2000) is used to follow the radial evolution of the secondary as

MB and GR shrink the orbit. The metallicity is set to the solar value of $Z = 0.02$. We neglect the evolutionary time prior to the SN of the primary and assume that the secondary is on the zero-age main sequence at the time the NS is formed. The age of the secondary when it fills its Roche lobe is here referred to as the "lag time," denoted by $t_{\rm lag}$. The lag time thus approximates the time between the formation of the primordial binary and the onset of the X-ray binary phase. We take the age of the Galaxy to be 13 Gyr and only accept as incipient L/IMXBs those for which $t_{\rm lag} < 13$ Gyr.

Figure 1 shows an illustrative set of distributions of binary parameters and systemic speeds for the incipient L/IMXBs. Overlaid on the scatter plots are the initial models (*open circles*) from our library of L/IMXBs evolutionary sequences. We applied fixed values of $y = 0.0$, $\sigma_k = 200$ km s^{-1}, $\eta_{\rm MB} = 1$ and considered CE structure parameters of $\lambda_{\rm CE} = \{0.1,\ 0.3,\ 0.5\}$. For each parameter set shown, the number of systems increases with secondary mass. This distribution is modified if we adopt a different distribution of mass ratios for the components of the primordial binaries. Nonetheless, the general statistical importance of initially intermediate-mass secondaries is clear. The high concentration of systems with $P_{\rm orb} \lesssim 0.5d$ and $M_d \lesssim 1.5$ when $\lambda_{\rm CE} = 0.3$ and 0.5 is due to MB and GR. The absence of LMXBs with evolved secondaries of mass $M_d \lesssim 1$ for $P_{\rm orb} \gtrsim 0.5$ days when $\lambda_{\rm CE} = 0.3$ and 0.5 results from the demand that $t_{\rm lag} < 13$ Gyr. More low-mass donors survive this cut if the metallicity is reduced, since the main-sequence lifetime decreases with decreasing metallicity. Note that for $\lambda_{\rm CE} = 0.1$, no systems with low-mass donors survive the CE and that the maximum period of the incipient IMXBs is only $\sim$3 days. When $\lambda_{\rm CE} = 0.1$, the small fraction of incipient IMXBs with $2.5 < M_d < 4$ is not well sampled by our grid of evolutionary sequences, but we expect that a denser sampling will not greatly change our results.

It is somewhat interesting that systems with fully convective secondaries of mass $M_d \lesssim 0.4$ can be driven into contact by GR within the lifetime of the Galaxy (eq. [8]). A handful of such binaries are present in Figure 1 for $\lambda_{\rm CE} = 0.3$ and 0.5. Mass transfer will be driven by GR at rates of $\lesssim 10^{-10}\ M_\odot$ yr^{-1}, from initial periods of $\sim$2–3 hr to a minimum period of $\sim$1.5 hr, at which point $M_d \sim 0.05$. The secondary and orbit then expand in response to further mass transfer. For a physical discussion of LMXB evolution with very low-mass donors and the period minimum, see Nelson, Rappaport, & Joss (1986). The companion mass ($M_d \gtrsim 0.04$) and orbital period ($P_{\rm orb} \simeq 2$ hr) of the first-discovered millisecond X-ray pulsar SAX J1808.4−3658 (Wijnands & van der Klis 1998; Chakrabarty & Morgan 1998) are consistent with it having formed and evolved in the way just described. However, given the uncertainty in the binary inclination, a model wherein the initial donor mass takes a more typical value of $\sim 1\ M_\odot$ is also consistent with the present system parameters (Nelson & Rappaport 2003).

We define the *formation efficiency* as $\mathscr{F}(<M_d) = N_{\rm inc}(<M_d)/{\rm N_{PB}}$, where $N_{\rm inc}(<M_d)$ is the synthesized number of incipient L/IMXBs with donor masses less than M_d, and $N_{\rm PB}$ is the number of primordial binaries used in the simulation. The majority of systems with $M_d > 4$ undergo dynamical mass transfer shortly after Roche lobe overflow (see Paper I). Therefore, we take $\mathscr{F}(<4)$ to be the *total* formation efficiency of LMXBs and IMXBs. We somewhat arbitrarily define incipient LMXBs as systems with initial donor masses of $M_d < 1.5$.

The present rate of core-collapse SNe in the Milky Way is $\mathscr{R}_{\rm SN} \sim 10^{-2}$ yr^{-1} (Cappellaro, Evans, & Turatto 1999). Here we adopt the simplifying assumption that the average star formation rate has been constant for 13 Gyr and take $R_{\rm SN}$ to be the approximate formation rate of massive primordial binaries. It follows that the current Galactic birthrate of L/IMXBs is $\mathscr{B}(<M_d) = \mathscr{F}(<M_d)\mathscr{R}_{\rm SN}$.

Table 1 lists formation efficiencies for a modest number of different parameter sets in the BPS study, where we vary only y, $\lambda_{\rm CE}$, σ_k, and $\eta_{\rm MB}$. We used 10^7 primordial binaries in each simulation. For the parameter sets explored, the formation efficiency of both LMXBs and IMXBs varies from $\log \mathscr{F}(<4) \simeq -4.1$ to -1.7, with corresponding birth rates of $\mathscr{B}(<4) \sim 10^{-6}$–$10^{-4}$ yr^{-1}. Incipient LMXBs are formed with systematically lower efficiencies of $\log \mathscr{F}(<1.5) \lesssim -2.4$ and birthrates of $\mathscr{B}(<1.5) \lesssim 4 \times 10^{-5}$ yr^{-1}. The range of LMXB birthrates is reasonably consistent with the results of, e.g., Portegies Zwart & Verbunt (1996) and Kalogera & Webbink (1998), each of whom used somewhat different assumptions than the ones adopted here. The formation efficiencies for $M_d < 0.4$ are also listed in Table 1, with typical values of $\log \mathscr{F}(<0.4) \lesssim -4$. If SAX J1808.4−3658 evolved from a system with such a low-mass secondary, then $\lambda_{\rm CE} \sim 0.5$ is favored, since this value yields the largest birthrates of $\mathscr{B}(<1.5) \sim 10^{-6}$ yr^{-1}.

4. POPULATION AT THE CURRENT EPOCH

In order to compare our theoretical population synthesis results and the statistics of observed systems, it is necessary to follow the evolution of each L/IMXB that we generate. For each synthesized system, a close match is found in our library of evolutionary sequences. Distributions at the current epoch of observable quantities are computed by appropriately weighting each evolutionary sequence. We now elaborate on these points and discuss several key results, as well as make very rudimentary comparisons between our results and the observations.

4.1. *Selection from the Library*

Each incipient L/IMXB is characterized by the donor mass and the circularized orbital period at which the star first fills its Roche lobe. For any given initial $P_{\rm orb}$ and M_d, we select a model from our L/IMXB evolutionary library by first identifying the subset of sequences in the library with the closest initial donor mass and then finding the one sequence in this subset with the closest initial orbital period. Incipient LMXBs with $M_d < 0.3$ are evolved by selecting the one sequence with an initial donor mass of 0.3 $M_\odot$ and considering only the part of the sequence for which the donor mass is less than M_d. This is reasonable, since such stars will initially follow the approximate mass-radius relation, $R_d \propto M_d^{0.8}$, for low-mass stars in thermal equilibrium. If the library sequences are labeled with some integer index i, we may define the formation efficiency $\mathscr{F}_i$ of sequence i as the number of times that sequence is selected, divided by $N_{\rm PB}$.

4.2. *Weighting Procedure*

For each selected library model, the entire evolutionary sequence contributes to the distributions at the current

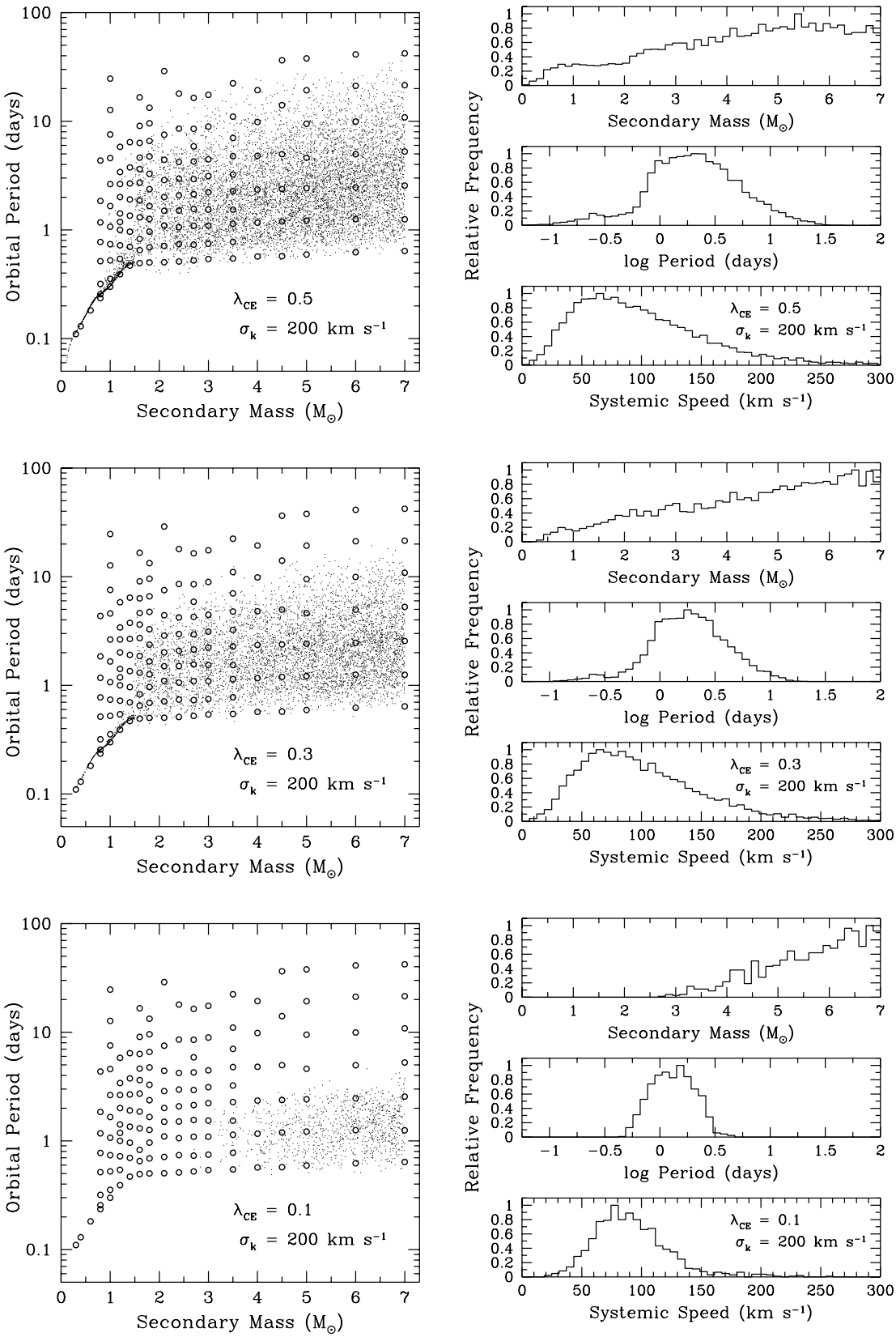

FIG. 1.—Scatter plots and histograms for incipient L/IMXBs. Each dot represents one binary system. For these simulations, we used 500,000 primordial binaries and parameter values of $y = 0.0$, $\sigma_k = 200$ km s^{-1}, $\eta_{\rm MB} = 1$, and $\lambda_{\rm CE} = \{0.1,\ 0.3,\ 0.5\}$. The clustering of systems with $P_{\rm orb} \lesssim 0.5d$ and $M_d \lesssim 1.5$ for $\lambda_{\rm CE} = 0.3$ and 0.5 is due to the effects of magnetic braking and gravitational radiation. The histograms also show the distributions of systemic speeds that result from the SNe. For reference, we have overlaid on the scatter plots the initial models in our library of evolutionary sequences (*open circles*).

TABLE 1
SELECTED RESULTS FROM OUR POPULATION STUDY

Model Number	y[a]	λ_{CE}[b]	η_{MB}[c]	σ_k[d]	log $\mathscr{F}(<4)$[e]	log $\mathscr{F}(<1.5)$	log $\mathscr{F}(<0.4)$	log N_X[f]	f_{SP}[g]	$\langle\tau_X\rangle$[h]
1	0.0	0.5	1.0	200	−2.17	−2.89	−3.99	4.52	0.36	5.03
2	0.0	0.5	1.0	100	−1.86	−2.60	−3.77	4.76	0.35	4.28
3	0.0	0.5	1.0	50	−1.70	−2.49	−3.84	4.83	0.35	3.53
4	0.0	0.3	1.0	200	−2.38	−3.22	−5.09	4.37	0.31	5.73
5	0.0	0.3	1.0	100	−2.06	−2.91	−5.00	4.62	0.30	4.91
6	0.0	0.3	1.0	50	−1.90	−2.74	−5.09	4.66	0.29	3.77
7	0.0	0.1	1.0	200	−3.87	<-7	<-7	2.84	0.30	5.23
8	0.0	0.1	1.0	100	−3.56	<-7	<-7	3.14	0.29	5.12
9	0.0	0.1	1.0	50	−3.41	<-7	<-7	3.30	0.23	5.33
10	0.0	0.5	0.0	200	−2.20	−3.04	−3.99	4.49	0.31	4.92
11	0.0	0.3	0.0	200	−2.40	−3.33	−5.09	4.35	0.27	5.73
12	0.0	0.1	0.0	200	−3.87	<-7	<-7	2.84	0.30	5.22
13	−1.0	0.5	1.0	200	−2.02	−2.38	−3.03	4.63	0.46	4.63
14	−1.0	0.3	1.0	200	−2.32	−2.81	−4.30	4.43	0.38	5.75
15	−1.0	0.1	1.0	200	−4.06	<-7	<-7	2.66	0.32	5.36
16	1.0	0.5	1.0	200	−2.56	−3.71	−5.52	4.06	0.29	4.30
17	1.0	0.3	1.0	200	−2.71	−3.98	−6.00	4.00	0.26	5.25
18	1.0	0.1	1.0	200	−4.06	<-7	<-7	2.62	0.29	5.14

[a] Exponent for the mass-ratio distribution.
[b] Binding-energy parameter for the common envelope ($\eta_{CE} = 1$; see text).
[c] Strength parameter for magnetic braking.
[d] Dispersion (in km s^{-1}) of the Maxwellian kick distribution.
[e] To obtain the approximate birthrates, multiply $\mathscr{F}$ by $\mathscr{R}_{SN} = 10^{-2}$ yr^{-1}.
[f] Total number of systems at the current epoch with $\dot{M}_a = 10^{-10}$–10^{-8} $M_\odot$ yr^{-1}.
[g] Fraction of short-period ($P_{orb} < 2$ hr) systems at the current epoch.
[h] Mean X-ray lifetime in units of 10^8 yr for $\dot{M}_a = 10^{-10}$–10^{-8} $M_\odot$ yr^{-1}.

epoch of P_{orb}, M_d, and $\dot{M}_a$, the accretion rate onto the NS. This is done as follows. Let Q be the quantity of interest. The evolutionary data file for each sequence gives Q as a function of the time t_{MT} since the onset of mass transfer to the NS. For some small interval of time δt_{MT}, Q varies over a small range $(Q, Q + \delta Q)$. The probability that there is an "identical" system that is *currently* in this particular state somewhere in the Galaxy is $\mathscr{F}_i \mathscr{R}_{SN}(t_{PB})\delta t_{MT}$, where $t_{PB} = -(t_{MT} + t_{lag})$ is the formation time of the primordial binary and *now* is taken to be at time $t = 0$. The total number of L/IMXBs present in the Galaxy with Q in the bin $(Q_0, Q_0 + \Delta Q)$ is $\sum \mathscr{F}_i \mathscr{R}_{SN}(t_{PB})\delta t_{MT}$. Here the symbolic sum is over all sequences i and all evolutionary times for which Q lies in the chosen bin. While the above procedure is valid for a variable star formation rate, we limit our study to a constant massive binary formation rate of $\mathscr{R}_{SN} = 10^{-2}$ yr^{-1} (see § 3).

4.3. *Current-Epoch Distributions*

Figure 2 shows theoretical distributions (*thin, solid histograms*) at the current epoch of M_d, P_{orb}, and $\dot{M}_a$, where we have used illustrative values of $y = 0.0$, $\sigma_k = 200$ km s^{-1}, and $\eta_{MB} = 1$. The left and right panels are for $\lambda_{CE} = 0.1$ and 0.5, respectively. Hatched regions indicate systems that are persistent X-ray sources (+45°) or transient (−45°; see below). The solid histogram that encloses the hatched regions shows the total number of systems. The dotted and thick, solid histograms in the right panel are explained in § 4.4 and § 5.2.

We decide if a system is persistent or transient according to the standard disk instability model (Cannizzo, Ghosh, & Wheeler 1982), wherein the accretion is transient if the X-ray irradiation temperature at the disk edge is $T_{irr} \gtrsim 10^4$ K (see van Paradijs 1996 and references therein), a characteristic hydrogen ionization temperature. The irradiation temperature at a radius R in the disk is given by (de Jong, van Paradijs, & Augusteijn 1996)

$$T_{irr}^4 = \frac{L_X}{4\pi\sigma_{SB}R^2}\frac{H}{R}(1-\gamma)(\xi-1)\,, \qquad (10)$$

where σ_{SB} is the Stefan-Boltzmann constant, H is the disk scale height at R, γ is the X-ray albedo of the disk, and $\xi \equiv d\ln H/d\ln R$. Following King, Kolb, & Burderi (1996), we take the outer disk radius to be 70% of the Roche lobe radius of the NS and adopt values of $\xi = \frac{9}{7}$ (Vrtilek et al. 1990), $\gamma = 0.9$, and $H/R = 0.2$ at the disk edge (de Jong et al. 1996). Fixing the NS mass and radius at 1.4 $M_\odot$ and 10 km, respectively, we find the following expression for the critical mass-transfer rate below which an L/IMXB is transient:

$$\frac{\dot{M}_{a,\mathrm{crit}}}{10^{-10}\ M_\odot\ \mathrm{yr}^{-1}} \sim (1+q)^{2/3} r_{La}^2 \left(\frac{P_{orb}}{1\ \mathrm{hr}}\right)^{4/3}\,, \qquad (11)$$

where r_{La} is the Roche lobe radius for the NS in units of the orbital separation. The value of $\dot{M}_{a,crit}$ is not certain to within a factor of at least a few, and so our numbers and distributions for transient and persistent systems should be considered cautiously.

In Figure 2, the shapes and extents of the theoretical distributions for $\lambda_{CE} = 0.1$ and 0.5 are quite similar. The most notable difference between the two cases is the total number of systems: $\sim 10^3$ when $\lambda_{CE} = 0.1$ and $\sim 10^5$ when $\lambda_{CE} = 0.5$. Also prominent in both panels are the very large number of systems with $P_{orb} \lesssim 2$ hr, the majority of which are transient

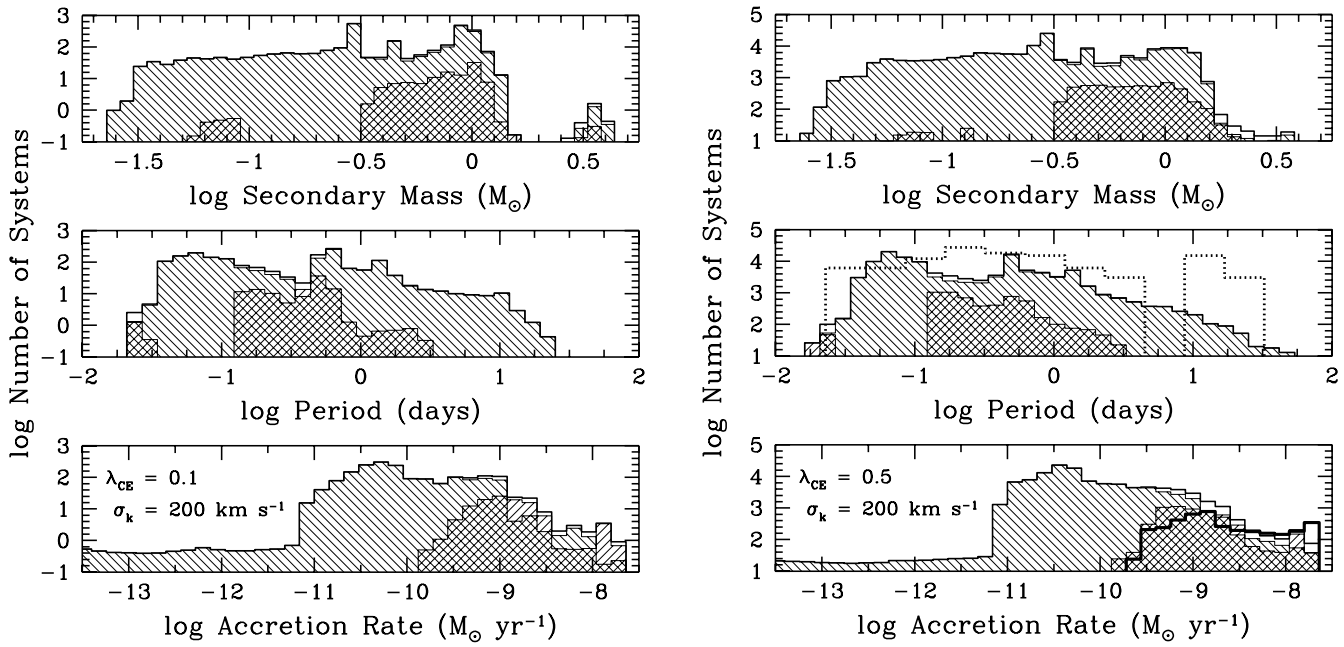

FIG. 2.—Distributions at the current epoch of the orbital period, donor mass, and mass accretion rate onto the NS, for parameters $y = 0.0$, $\sigma_k = 200$ km s^{-1}, $\eta_{MB} = 1$, and $\lambda_{CE} = 0.1$ (*left*) and 0.5 (*right*). We have assumed a constant massive binary formation rate of 10^{-2} yr^{-1}. Note the difference in scale between the left and right figures. The hatched regions indicate persistent (+45°) and transient (−45°) X-ray sources, and the enclosing solid histogram gives the sum of these two populations. Overlaid (*dotted histogram*) on the theoretical period distribution in the figure on the right is the rescaled distribution of 37 measured periods (Liu et al. 2001) among ~140 observed LMXBs in the Galactic plane. The thick, solid distribution overlaid on the bottom panel of the right figure illustrates how the inclusion of X-ray irradiation effects might change our theoretical $\dot{M}_a$ distribution.

according to equation (11). Note finally that, while IMXBs are much more favorably produced than LMXBs, very few systems at the current epoch have donors of mass greater than 1 $M_\odot$. This is simply because the initial phase of thermal-timescale mass transfer in IMXBs, where a large fraction of the secondary mass is removed, is relatively short-lived (see Fig. 2*a* of Paper I).

4.4. *Comparisons with Observation*

Small number statistics, observational selection effects, and sample incompleteness are all serious issues for the observed LMXBs. Out of ~140 Galactic X-ray sources classified as LMXBs with NS accretors, there are only ~40 systems in the Galactic disk with measured orbital periods and a handful with estimated secondary masses. Usually, the nondetection of the donor at optical wavelengths is taken to mean that it is of low mass. The estimation of X-ray luminosities among the observed LMXBs outside of globular clusters is typically complicated by poor distance estimates. Furthermore, for X-ray luminosities less than $L_X \sim 10^{36}$ ergs s^{-1} ($\dot{M}_a \sim 10^{-10}\ M_\odot$ yr^{-1}), the observed sample may be quite incomplete. Even in light of these problems, rough comparisons between our theoretical results and the observations are illuminating. The most apparent quantitative discrepancy is in the total numbers of systems.

We define N_X to be the total number of L/IMXBs at the current epoch—both persistent and transient—with secular accretion rates of $\dot{M}_a > 10^{-10}\ M_\odot$ yr^{-1}. Thus, N_X quantifies the number of *luminous* X-ray binaries likely to be observed over a large fraction of the Galactic volume. Table 1 lists values of $\log N_X$ for different parameter sets, from which we see that N_X ranges from ~3 to more than 400 times the total of ~140 systems observed in the Galaxy. We elaborate in the next section on this rather severe overproduction problem.

In Figure 2, for $\lambda_{CE} = 0.5$, we have overlaid (*dotted histogram*) the distribution of 37 measured orbital periods for LMXBs outside of globular clusters (Liu et al. 2001), which has been multiplied by a factor of 3000 for comparison purposes. With such small numbers (1–9) per bin, meaningful comparisons with our theoretical distribution are difficult. It may be that we are underproducing systems with $P_{orb} \gtrsim 10$ days and overproducing short-period LMXBs with $P_{orb} \lesssim 0.1$ days. Our simulations indicate that most of the short-period systems are transient, which may aid in explaining a possible discrepancy. Furthermore, binaries with $P_{orb} \lesssim 2$ hr are driven by GR with characteristically low X-ray luminosities of $L_X < 10^{35}$–10^{36} ergs s^{-1}, making them more difficult to discover. We compute the fraction, f_{SP}, of short-period ($P_{orb} < 2$ hr) LMXBs at the current epoch and find that, typically, $f_{SP} \sim 0.3$ (Table 1), which in itself is not in serious conflict with observations, for reasons already mentioned.

In our simulations, we actually underestimate the number of short-period ($P_{orb} \lesssim 2$ hr) LMXBs at the current epoch. These binaries evolve from systems with initial orbital periods below the bifurcation period of ~18 hr found in Paper I and reach minimum periods of ~10 minutes to ~1.5 hr. For technical reasons, our X-ray binary calculations are terminated not long after the minimum period is reached. The subsequent evolution is driven by GR at low rates but may last for billions of years. This makes the discrepancy with the observations somewhat worse. On the other hand, we note that three ultracompact binary systems have been discovered within the past year alone, so the discovery probability for these systems may be increasing.

The value of the bifurcation period is rather uncertain and depends on metallicity (Burderi, D'Antona, & Burgay

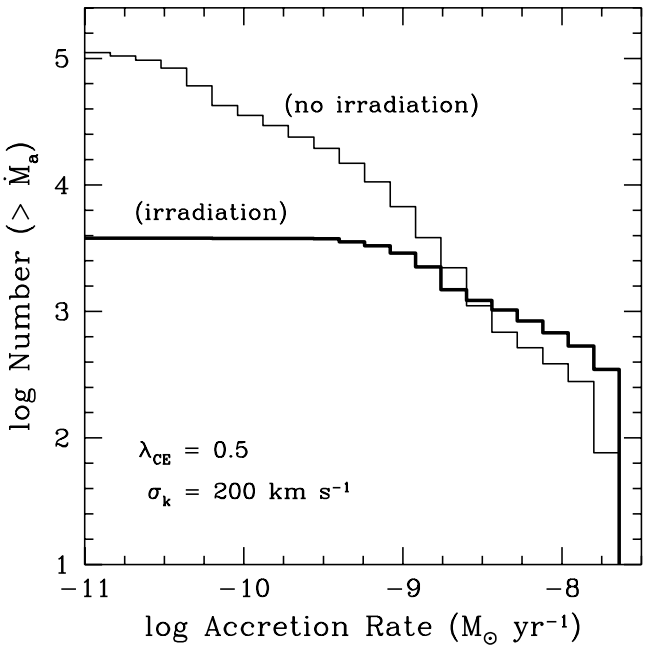

FIG. 3.—Cumulative distribution of accretion rates at the current epoch for the same systems used to generate Fig. 2 ($\lambda_{CE} = 0.5$). Here we include both persistent and transient systems. The thick line corresponds to our ad hoc inclusion of irradiation effects.

2002), systemic mass loss (Ergma 1996; Ergma & Sarna 1996), and the prescription for magnetic braking (Pylyser & Savonije 1988). In particular, if the strength of magnetic braking is significantly reduced, the bifurcation period may approach ~10 hr (see, e.g., Paper I), thus reducing the number of short-period binaries and increasing the number of L/IMXBs that evolve to long periods. This, of course, impacts our calculated distribution of L/IMXB orbital periods and is especially important for the production of BMPs and their orbital-period distribution (see § 5.1). The role of the bifurcation period for the formation and evolution of L/IMXBs and the production of BMPs should be investigated more systematically in the future.

Extrapolating the data available for 16 Galactic LMXBs monitored by *RXTE*/ASM, Grimm, Gilfanov, & Sunyaev (2002) have attempted to compute a cumulative X-ray luminosity distribution, corrected for the fraction of the Galactic volume observable by the ASM. For luminosities of $\gtrsim 10^{36}$ ergs s^{-1}, we expect that the observed sample should be reasonably complete. As a point of comparison, we have chosen to compute the ratio of the number of LMXBs with X-ray luminosities of $L_X = 10^{36}$–10^{37} ergs s^{-1} to the number with $L_X > 10^{37}$ ergs s^{-1}. The results of Grimm et al. (2002) indicate that this ratio is ~1.5. Our theoretical cumulative distribution of mass accretion rates is shown as the thin line in Figure 3; the thick line will be discussed in § 5.2. For the two luminosity ranges given above, we find a larger number ratio of ~5.3. It is not clear if this particular discrepancy between our theoretical results and the observations is especially significant.

5. DISCUSSION

In this section, we devote a short discussion to each of three important topics that relate to L/IMXB evolution. Binary millisecond pulsars are discussed, with emphasis on the orbital period distribution and the long-standing birthrate problem. We also address the possible importance of X-ray irradiation of the donor stars in L/IMXBs. Finally, we briefly investigate the possibility of forming low-mass black holes in L/IMXBs via accretion-induced collapse.

5.1. *Binary Millisecond Radio Pulsars and the Birthrate Problem*

Binary millisecond radio pulsars (BMPs) are widely thought to be the evolutionary descendants of L/IMXBs (Alpar et al. 1982; Joss & Rappaport 1983). Using our BPS code and library of evolutionary sequences, we compute the orbital period distribution of BMPs in the following way. Most sequences are terminated after the He or HeCO white-dwarf core of the donor star is exposed (see Paper I). For the binaries that contract to $P_{orb} \lesssim 2$ hr, the evolution ends not long after the period minimum is reached; as mentioned above, further evolution to longer periods is not followed. We do not consider the effects of pulsar turn-on on the evolution of the binary (see, e.g., Burderi et al. 2002). At the end of each sequence, we know the orbital period and mass of the secondary. Each sequence i and the corresponding final orbital period are weighted by the formation efficiency $\mathscr{F}_i$, and the results are accumulated to generate a histogram. We have not attempted to include any estimates for the pulsar lifetime or detectability in our analysis.

Two examples of the calculated orbital-period distribution are shown in Figure 4 (*solid histograms*), where $y = 0.0$, $\eta_{MB} = 1.0$, $\sigma_k = 200$ km s^{-1}, and $\lambda_{CE} = 0.1$ and 0.5. Systems in Figure 4 with $P_{orb} \lesssim 2$ hr are meant only to indicate the relative proportions of short-period and long-period BMPs produced in our simulations. Of course, this proportion and the distribution as a whole will be modified if the bifurcation period changes because of different assumptions about the stellar metallicity, systemic mass loss, or magnetic braking (see § 4.4). Overlaid on each panel in Figure 4 is the period distribution of the observed systems (*dashed histogram*; taken from Taam, King, & Ritter 2000). Both distributions are normalized to unit area. Clearly, neither parameter set adequately reproduces the observed distribution, and the agreement is extremely poor for $\lambda_{CE} = 0.1$. Larger values of λ_{CE} are strongly favored, since L/IMXBs form over a much wider range of initial periods and donor masses (see Fig. 1, *top panels*) than when $\lambda_{CE} \sim 0.1$, which results in a wider range of BMP orbital periods. The same conclusion was reached by Willems & Kolb (2002), who used simplified models of L/IMXB evolution in a focused population synthesis study of BMPs. However, $\lambda_{CE} \sim 0.5$ is problematic, since the number of luminous L/IMXBs at the current epoch is greatly overproduced in our models by factors of $\gtrsim 100$, relative to the observed number, as noted in the last section. This problem emerges again when one considers the birthrates of BMPs based on the observed sample.

Lorimer (1995) and Cordes & Chernoff (1997) each conservatively estimate the total Galactic birthrate of BMPs to be $\sim 10^{-6}$ yr^{-1}. Their likelihood analyses considered ~20 BMPs and included known pulsar selection effects, a model for the spatial distribution of BMPs, and estimated distance errors. Lorimer (1995) notes that several uncertainties may increase the birthrate by a factor of 10, to $\sim 10^{-5}$ yr^{-1}. In addition, the pulsar spin-down ages used in these studies may systematically overestimate the true ages of the systems (Lorimer 1995; Hansen & Phinney 1998), leading to larger actual birthrates. Given the ~100 observed LMXBs in the

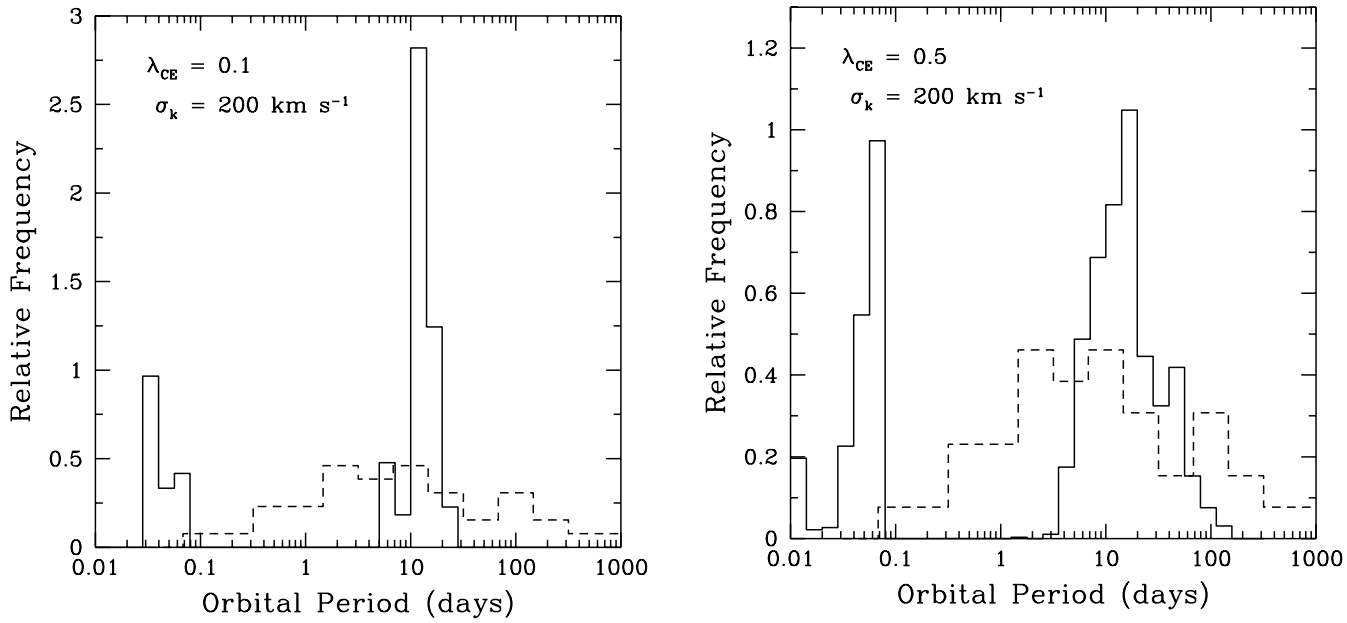

FIG. 4.—Orbital period distribution of binary millisecond radio pulsars. The solid and dashed histograms are for the theoretical and observed systems, respectively. Both distribution are normalized to unit area.

Galaxy and a typical observable X-ray lifetime of $\langle\tau_X\rangle \sim 10^9$ yr, the semiempirical birthrate of LMXBs is $\sim 10^{-7}$ yr^{-1}, which is 10–100 times lower than the BMP birthrate. Kulkarni & Narayan (1988) were the first to point out this potentially important discrepancy.

Recall from § 3 that the model birthrates of L/IMXBs lie in the range $\sim 10^{-6}$–10^{-4} yr^{-1}, which covers the range of semiempirical BMP birthrates. The largest L/IMXB birthrates, which may be required if the BMP birthrate is $\sim 10^{-5}$ yr^{-1}, result from $\lambda_{CE} \sim 0.3$–0.5, which, in turn, yields far too many luminous X-ray sources at the current epoch. Although the active X-ray lifetime is not relevant for our theoretical L/IMXB birthrate calculations, this is an important quantity to calculate.

We define the mean *luminous* X-ray lifetime from our simulations to be

$$\langle\tau_X\rangle = \sum \mathscr{F}_i \Delta t_i \Big/ \sum \mathscr{F}_i \, , \qquad (12)$$

where Δt_i is the total time spent by sequence i in the interval $\dot{M}_a > 10^{-10}\ M_\odot$ yr^{-1}, and the sum is over all sequences with $M_d < 4$ selected in the population synthesis calculation. We have not attempted to correct $\langle\tau_X\rangle$ for systems that are transient according to the disk instability model, since the transient duty cycle is unknown. From Table 1, we see that $\langle\tau_X\rangle$ is consistently $\sim 5 \times 10^8$ yr. This justifies the past use of $\langle\tau_X\rangle \sim 10^9$ yr as a typical LMXB lifetime. However, it is essentially this long X-ray lifetime that yields such large numbers of luminous sources at the current epoch in our model calculations. We now discuss a possible resolution to this serious conflict.

5.2. *Irradiation-Induced Mass-Transfer Cycles*

Our binary evolution calculations do not account for X-ray irradiation effects on the secondary, which can dramatically change the evolution of the system, either by driving winds (Ruderman, Shaham, & Tavani 1989) or the expansion of the star (Podsiadlowski 1991). Cyclic mass transfer may result from the irradiation, characterized by short episodes of enhanced mass transfer and long detached phases (Hameury et al. 1993; Harpaz & Rappaport 1994). Such cycles may then significantly reduce the total X-ray active lifetime, and thus resolve the L/IMXB overproduction problem and the discrepancy between the semiempirical birthrates of BMPs and LMXBs.

X-ray irradiation affects stars of mass $\lesssim 1.5\ M_\odot$ by ionizing the hydrogen at the base of the irradiated surface layer and disrupting the surface convection zone. By changing the surface boundary condition in this way, the star would tend to expand to a new thermal-equilibrium radius (Podsiadlowski 1991), with more dramatic expansion as the total stellar mass is decreased and the fractional mass in the surface convection zone is increased. Intermediate-mass stars in IMXBs, which are initially fully radiative, may be strongly affected by irradiation once the mass is reduced to $\lesssim 1$–$1.5\ M_\odot$ and a surface convection zone appears, after the early, rapid phase of thermal-timescale mass transfer. The detailed role of irradiation in X-ray binary evolution is rather poorly understood (some important uncertainties are discussed in Harpaz & Rappaport 1991, 1995; Hameury et al. 1993). Importantly for our study, it is not known how irradiation influences the evolution of red giants. The subject of irradiation in close binary systems is a major long-term research project of one of the authors (see Phillips & Podsiadlowski 2002; Beer & Podsiadlowski 2002a, 2002b). A related problem, which we do not consider here, is how pulsar irradiation influences the structure of the secondary and the mechanism by which an L/IMXB ultimately turns on as a binary millisecond radio pulsar (Burderi et al. 2002).

An irradiation temperature of $\gtrsim 10^4$ K, a characteristic ionization temperature for hydrogen, gives a critical X-ray flux of $S_c \sim 10^{11}$–10^{12} ergs s^{-1} cm^{-2}, above which irradiation is important. Letting $S_{c,11}$ be the critical flux in units of

10^{11} ergs s^{-1} cm^{-2} and $\dot{M}_{a,-8}$ be the accretion rate onto the NS in units of 10^{-8} $M_\odot$ yr^{-1}, we estimate the maximum orbital period for which irradiation is important,

$$P_{\rm orb} \sim 70 \text{ days } \left(\frac{\epsilon\, \dot{M}_{a,-8}}{S_{c,11}}\right)^{3/4}, \qquad (13)$$

where $\epsilon < 1$ is a factor that takes into account the geometry of the accretion disk and star, albedo of the star, and fraction of X-rays that penetrate below the stellar photosphere (Hameury et al. 1993). It is at least plausible, and perhaps likely, that X-ray irradiation significantly alters the evolution of most L/IMXBs.

When irradiation effects are relatively moderate, the results of Hameury et al. (1993) indicate that irradiation-induced mass-transfer cycles do not typically change the secular evolution of $P_{\rm orb}$ or M_d. Therefore, at least in this limit, we can use our grid of evolutionary sequences to investigate the effects of irradiation cycles, since our models describe the secular evolution of $P_{\rm orb}$ or M_d approximately correctly. Under these circumstances, the inclusion of irradiation would not change the $P_{\rm orb}$ and M_d distributions in Figure 2. However, the distribution of $\dot{M}_a$ would change significantly. Suppose that the donors in all L/IMXBs are affected by irradiation in essentially the same way, such that the mass-transfer rate is on average enhanced by a factor of $f_{\rm en} > 1$ during episodes of Roche lobe overflow. We then expect the $\log \dot{M}_a$ distribution in Figure 2 to be shifted to the right by an amount $\log f_{\rm en}$ but still cut off at the Eddington limit. Furthermore, the distribution is everywhere decreased in height by an amount $-\log f_{\rm en}$, since the X-ray lifetime for each system is reduced by a factor $f_{\rm en}^{-1}$. In order to alleviate the L/IMXB overproduction problem and the BMP birthrate problem, we perhaps need to have $\langle \tau_{\rm X} \rangle$ reduced by a factor of $\gtrsim$100. This would require $f_{\rm en} \gtrsim 100$, depending on the shape of the $\dot{M}_a$ distribution calculated *without* irradiation.

In Figures 2 ($\lambda_{\rm CE} = 0.5$) and 3, we have overlaid (*thick, solid histogram*) a distribution that may very roughly illustrate the net effects of irradiation for an illustrative enhancement factor of $f_{\rm en} = 30$. To get this result, we simply multiplied the mass-transfer rate from the donor by $f_{\rm en}$ and all times by $f_{\rm en}^{-1}$ in each of the selected evolutionary sequences, regardless of the instantaneous values of M_d or $P_{\rm orb}$. We have chosen $f_{\rm en} = 30$, since it happens that $\langle \tau_{\rm X} \rangle$ and $N_{\rm X}$ are reduced by a factor of $\simeq$10. We emphasize that irradiation effects have not been incorporated self-consistently into our L/IMXB evolutionary sequences, and our approach is only meant to gauge the possible effects of irradiation on the population of L/IMXBs. The resulting $\dot{M}_a$ distribution (Fig. 2) is confined to the range $\dot{M}_a > 10^{-10}$ $M_\odot$ yr^{-1}, and we find that most of these systems are persistent. From the corresponding cumulative distribution shown in Figure 3, we find that the ratio of the number of LMXBs with luminosities of 10^{36}–10^{37} ergs s^{-1} to the number with $L_{\rm X} > 10^{37}$ ergs s^{-1} is $\sim$0.6, smaller than the observed value (see § 4.4). However, irradiation effects at least produce the desired outcome of reducing this ratio from our earlier quoted theoretical value of $\sim$5.3.

5.3. *Low-Mass Black Holes*

It is generally assumed that an NS cannot accrete at rates exceeding the Eddington limit ($\dot{M}_{\rm Edd} \sim 10^{-8}$ $M_\odot$ yr^{-1}).

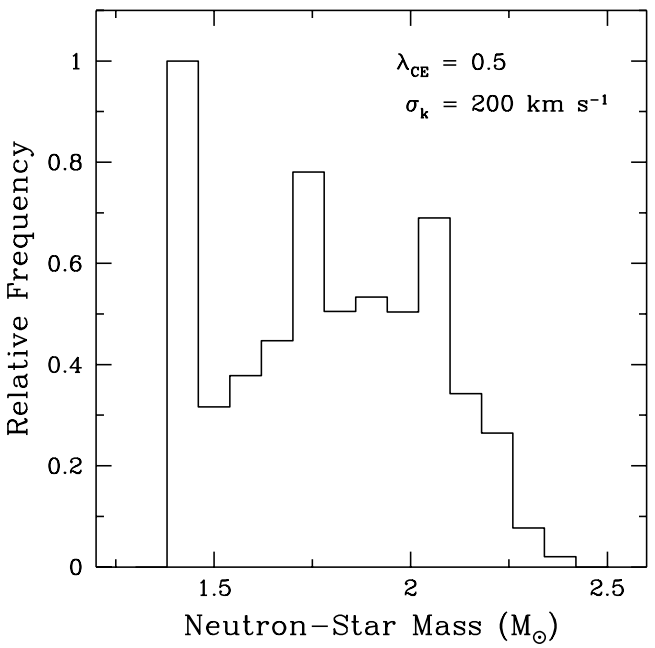

FIG. 5.—Distribution of final NS masses for BPS parameters $y = 0.0$, $\eta_{\rm MB} = 1$, $\sigma_k = 200$ km s^{-1}, and $\lambda_{\rm CE} = 0.5$.

Material donated faster than $\dot{M}_{\rm Edd}$, e.g., during thermal-timescale mass transfer, will likely be ejected from the system, possibly as a radiatively driven wind from the accretion disk or in the form of relativistic jets. Evidence for both of these processes is seen in the X-ray binary SS 433 (Blundell et al. 2001), a system known to be in a phase of super-Eddington mass transfer.

Our library of evolutionary sequences was computed with one reasonable, though heuristic, prescription for the mass capture fraction β,

$$\beta = \begin{cases} b\,, & |\dot{M}_2| < \dot{M}_{\rm Edd}\,, \\ b\ \dot{M}_{\rm Edd}/|\dot{M}_2|\,, & |\dot{M}_2| > \dot{M}_{\rm Edd}\,, \end{cases} \qquad (14)$$

where $b \leq 1$ is a constant. This formula limits the accretion rate to be $\dot{M}_a < b\ \dot{M}_{\rm Edd}$. We used a specific value of $b = 0.5$ in our calculations.

The distribution of final NS masses (Fig. 5) was computed in the same way as the orbital-period distribution for BMPs. Masses up to $\sim$2.5 $M_\odot$ were reached in these simulations. Modern NS equations of state give maximum masses of $\simeq$1.8–2.5 $M_\odot$ (Akmal, Pandharipande, & Ravenhall 1998). Thus, even for $b = 0.5$, it is possible that a significant fraction of L/IMXBs ultimately contain a low-mass black hole. If we had used $b = 1$, our NS mass distribution would have broadened to include masses up to $\sim$3.6 $M_\odot$, and perhaps more than half of the NSs in L/IMXBs would collapse to black holes. Such systems would not exhibit X-ray bursts and are unlikely to show the twin kHz quasi-periodic oscillations seen in LMXBs (van der Klis 2000). The inclusion of X-ray irradiation on the donor star, and the possible dramatic decrease in the X-ray lifetime, may generally yield final NS masses much closer to the initial mass of 1.4 $M_\odot$. Perhaps this could explain why the measured NS masses in BMPs are near $\sim$1.4 $M_\odot$ (Thorsett & Chakrabarty 1999).

6. SUMMARY AND OUTLOOK

Here we list the key points and results of this paper, in decreasing order of importance.

1. This is the first population synthesis study of L/IMXBs that incorporates detailed evolutionary calculations. With this addition, we are able to follow a population of L/IMXBs (*a*) from the incipient stage, (*b*) to the current epoch, and finally, (*c*) to the remnant state when they presumably become BMPs. We are thus able to meaningfully compare our results with the sample of observed LMXBs and BMPs.

2. We have demonstrated that incipient IMXBs outnumber incipient LMXBs typically by a factor of $\gtrsim 5$ (see Table 1). Since IMXBs may evolve to resemble observed LMXBs, we claim that the majority of observed systems may have started their lives with intermediate-mass donor stars.

3. We find that rather large values of $\lambda_{\rm CE}$ (~ 0.5) are required in order (*a*) for the theoretical BMP $P_{\rm orb}$ distribution to even remotely resemble the observed distribution, and (*b*) to yield L/IMXB birthrates that are consistent with the semiempirical BMP birthrates. However, we have discovered that such values of $\lambda_{\rm CE}$ lead to a dramatic overproduction of the number of luminous X-ray binaries in the Galaxy at the current epoch, by factors of $\gtrsim 100$.

4. The overproduction problem and the discrepancy between semiempirical BMP and LMXB birthrates may be resolved if the mean X-ray lifetime of L/IMXBs is reduced by a factor of $\gtrsim 100$. Cyclic mass transfer, induced by the X-ray irradiation of the donor star, may have the desired outcome. X-ray irradiation might strongly affect the evolution of most L/IMXBs. Although we take seriously the proposition that X-ray irradiation effects might go a long way toward resolving several important problems in the theory of L/IMXB formation and evolution, the self-consistent inclusion of X-ray irradiation at a level that can modify by a factor of $\gtrsim 100$ the lifetime of the X-ray active phase remains an important open problem and future goal.

5. Eddington-limited accretion onto the NS can lead to large NS masses of ~ 2–$4\ M_\odot$. It is then possible that a significant fraction of NSs in L/IMXBs collapse to low-mass black holes. To our knowledge, the only way to confirm the presence of a low-mass black hole in an observed LMXB is to measure the mass dynamically, which is extremely difficult in general. On the other hand, if the X-ray lifetimes of L/IMXBs are reduced substantially, by, e.g., the effects of X-ray irradiation, so too is the amount of mass that NSs can accrete. This may also explain why the measured NS masses in observed BMPs lie near $\sim 1.4\ M_\odot$.

We conclude by listing a number of ways that our work may be extended and improved.

1. Since X-ray irradiation of the donor star may be an extremely important component of L/IMXB evolution, it is important to have a better quantitative understanding of this process. The problem is inherently three-dimensional and must be treated as such in order to obtain meaningful quantitative results. Important first steps in this regard have been made by Phillips & Podsiadlowski (2002) and Beer & Podsiadlowski (2002a, 2002b), but much work remains to be done.

2. A detailed comparison of theoretical models of L/IMXBs formation and evolution with the observed population requires that we compute the spatial trajectories of the synthesized systems in a realistic Galactic gravitational potential. It then becomes possible to generate theoretical X-ray flux distributions as well as distributions in Galactic latitude and longitude. A treatment of observational selection effects, such as instrumental flux limits and X-ray absorption, also becomes possible.

3. Our library of L/IMXB evolutionary sequences will soon be incorporated into a sophisticated dynamical Monte Carlo code to study the evolution of globular clusters (Fregeau et al. 2003 and references therein). The code now incorporates direct numerical integrations of single-binary and binary-binary dynamical interactions, a mass spectrum of stars, and analytic treatments of single-star evolution. The inclusion of our library of X-ray binary calculations will make it possible to study directly the LMXB and BMP populations in globular clusters.

4. An appropriately detailed treatment of the tidal evolution of incipient L/IMXBs immediately after the SN should be included in future studies. Orbital circularization and spin synchronization of the secondary, coupled with orbital angular momentum loss due to GR as well the loss of spin angular momentum that results from MB should be considered.

5. It would be extremely advantageous if L/IMXB evolutionary calculations could be carried out at least 100 times faster than is possible at present. On a reasonably fast workstation, a typical computing time is currently ~ 20 minutes, so that, realistically, several days of computing time would be required to regenerate our current library of sequences. The development of an ultrafast Henyey-type stellar evolution code, along with increased processor speed over the next several years, may make it possible to carry out 1000 L/IMXB evolutions in ~ 10 hr of computing time.

E. P. was supported by NASA and the Chandra Postdoctoral Fellowship program through grant number PF2-30024, awarded by the Chandra X-Ray Center, which is operated by the Smithsonian Astrophysical Observatory for NASA under contract NAS8-39073. S. R. acknowledges some support from NASA ATP grant NAG5-12522.

REFERENCES

Abt, H. A., & Levy, S. G. 1978, ApJS, 36, 241
Akmal, A., Pandharipande, V. R., & Ravenhall, D. G. 1998, Phys. Rev. C, 58, 1804
Alpar, M. A., Cheng, A. F., Ruderman, M. A., & Shaham, J. 1982, Nature, 300, 728
Arzoumanian, Z., Chernoff, D. F., & Cordes, J. M. 2002, ApJ, 568, 289
Beer, M. E., & Podsiadlowski, Ph. 2002a, MNRAS, 335, 358
———. 2002b, in ASP Conf. Ser. 279, Exotic Stars as Challenges to Evolution, ed. C. Tout & W. Van Hamme (San Francisco: ASP), 253
Belczynski, K., Kalogera, V., & Bulik, T. 2002, ApJ, 572, 407
Blaauw, A. 1961, Bull. Astron. Inst. Netherlands, 15, 265
Blundell, K. M., Mioduszewski, A. J., Muxlow, T. W. B., Podsiadlowski, Ph., & Rupen, M. P. 2001, ApJ, 562, L79
Boersma, J. 1961, Bull. Astron. Inst. Netherlands, 15, 291
Brown, G. E., Heger, A., Langer, N., Lee, C.-H., Wellstein, S., & Bethe, H. A. 2001, NewA, 6, 457
Burderi, L., D'Antona, F., & Burgay, M. 2002, ApJ, 574, 325
Cannizzo, J. K., Ghosh, P., & Wheeler, J. C. 1982, ApJ, 260, L83
Cappellaro, E., Evans, R., & Turatto, M. 1999, A&A, 351, 459
Chakrabarty, D., & Morgan, E. H. 1998, Nature, 394, 346
Cordes, J. M., & Chernoff, D. F. 1997, ApJ, 482, 971
De Greve, J.-P., & De Loore, C. 1977, Ap&SS, 50, 75

de Jong, J. A., van Paradijs, J., & Augusteijn, T. 1996, A&A, 314, 484
Delgado, A. J., & Thomas, H.-C. 1981, A&A, 96, 142
Dewi, J. D. M., Pols, O. R., Savonije, G. J., & van den Heuvel, E. P. J. 2002, MNRAS, 331, 1027
Dewi, J. D. M., & Tauris, T. M. 2000, A&A, 360, 1043
———. 2001, in ASP Conf. Ser. 229, Evolution of Binary and Multiple Star Systems, ed. Ph. Podsiadlowski, S. Rappaport, A. R. King, F. D'Antona, & L. Burderi (San Francisco: ASP), 255
Ergma, E. 1996, A&A, 315, L17
Ergma, E., & Sarna, M. J. 1996, MNRAS, 280, 1000
Fregeau, J. M., Gurkan, M. A., Joshi, K. J., & Rasio, F. A. 2003, ApJ, in press
Garmany, C. D., Conti, P. S., & Massey, P. 1980, ApJ, 242, 1063
Grimm, H.-J., Gilfanov, M., & Sunyaev, R. 2002, A&A, 391, 923
Habets, G. M. H. J. 1986a, A&A, 165, 95
———. 1986b, A&A, 167, 61
Hameury, J. M., King, A. R., Lasota, J. P., & Raison, F. 1993, A&A, 277, 81
Hansen, B. M. S., & Phinney, E. S. 1997, MNRAS, 291, 569
———. 1998, MNRAS, 294, 569
Harpaz, A., & Rappaport, S. 1991, ApJ, 383, 739
———. 1994, ApJ, 434, 283
———. 1995, A&A, 294, L49
Hurley, J. R., Pols, O. R., & Tout, C. A. 2000, MNRAS, 315, 543
Ivanova, N., Belczynski, K., Kalogera, V., Rasio, F. A., & Taam, R. E. 2003, ApJ, 592, 475
Joss, P. C., & Rappaport, S. A. 1983, Nature, 304, 419
Kalogera, V. 1998, ApJ, 493, 368
Kalogera, V., & Webbink, R. F. 1996, ApJ, 458, 301
———. 1998, ApJ, 493, 351
King, A. R., Kolb, U., & Burderi, L. 1996, ApJ, 464, L127
King, A. R., & Ritter, H. 1999, MNRAS, 309, 253
Kippenhahn, R., & Weigert, A. 1967, Z. Astrophys., 65, 251
Kolb, U., Davies, M. B., King, A., & Ritter, H. 2000, MNRAS, 317, 438
Kroupa, P., Tout, C. A., & Gilmore, G. 1993, MNRAS, 262, 545
Kulkarni, S. R., & Narayan, R. 1988, ApJ, 335, 755
Langer, N., & Maeder, A. 1995, A&A, 295, 685
Liu, Q. Z., van Paradijs, J., & van den Heuvel, E. P. J. 2001, A&A, 368, 1021
Lorimer, D. R. 1995, MNRAS, 274, 300
Miller, G. E., & Scalo, J. M. 1979, ApJS, 41, 513
Nelson, L. A., & Rappaport, S. A. 2003, ApJ, submitted (astro-ph/0304374)
Nelson, L. A., Rappaport, S. A., & Joss, P. C. 1986, ApJ, 304, 231
Pfahl, E., Rappaport, S., & Podsiadlowski, Ph. 2002, ApJ, 573, 283
Phillips, S. N., & Podsiadlowski, Ph. 2002, MNRAS, 337, 431
Podsiadlowski, Ph. 1991, Nature, 350, 136
Podsiadlowski, Ph., Joss, P. C., & Hsu, J. J. L. 1992, ApJ, 391, 246
Podsiadlowski, Ph., & Rappaport, S. 2000, ApJ, 529, 946
Podsiadlowski, Ph., Rappaport, S., & Han, Z. 2003, MNRAS, 341, 385
Podsiadlowski, Ph., Rappaport, S., & Pfahl, E. D. 2002, ApJ, 565, 1107
Pols, O. R. 1994, A&A, 290, 119
Pols, O. R., & Dewi, J. D. M. 2002, Publ. Astron. Soc. Australia, 19, 233
Portegies Zwart, S. F., & Verbunt, F. 1996, A&A, 309, 179
Pylyser, E., & Savonije, G. J. 1988, A&A, 191, 57
Rappaport, S., Joss, P. C., & Verbunt, F. 1983, ApJ, 275, 713
Rappaport, S., Joss, P. C., & Webbink, R. F. 1982, ApJ, 254, 616
Ruderman, M., Shaham, J., & Tavani, M. 1989, ApJ, 336, 507
Scalo, J. M. 1986, Fundam. Cosmic Phys., 11, 1
Shirey, R. E. 1998, Ph.D. thesis, Massachusetts Institute of Technology
Taam, R. E., King, A. R., & Ritter, H. 2000, ApJ, 541, 329
Tauris, T. M., & Savonije, G. J. 1999, A&A, 350, 928
Tauris, T. M., van den Heuvel, E. P. J., & Savonije, G. J. 2000, ApJ, 530, L93
Thorsett, S. E., & Chakrabarty, D. 1999, ApJ, 512, 288
van der Klis, M. 2000, ARA&A, 38, 717
van Paradijs, J. 1996, ApJ, 464, L139
Verbunt, F., & Zwaan, C. 1981, A&A, 100, L7
Vrtilek, S. D., Raymond, J. C., Garcia, M. R., Verbunt, F., Hasinger, G., & Kurster, M. 1990, A&A, 235, 162
Webbink, R. F. 1984, ApJ, 277, 355
Wellstein, S., Langer, N., & Braun, H. 2001, A&A, 369, 939
Wijnands, R., & van der Klis, M. 1998, Nature, 394, 344
Willems, B., & Kolb, U. 2002, MNRAS, 337, 1004